IOP Publishing Superconductor Science and Technology
Supercond. Sci. Technol. 31 (2018) 055005 (9pp) https://doi.org/10.1088/1361-6668/aab58c

Viscous flux flow velocity and stress distribution in the Kim model of a long rectangular slab superconductor

Yong Yang[1,2] **and Xueguang Chai**[1]

[1] School of Mechano-Electronic Engineering, Xidian University, Xi'an 710071, People's Republic of China
[2] Superconducting Materials Research Center, Northwest Institute for Nonferrous Metal Research, Xi'an 710016, People's Republic of China

E-mail: yangyong@xidian.edu.cn

Received 8 January 2018, revised 6 March 2018
Accepted for publication 9 March 2018
Published 29 March 2018

Abstract

When a bulk superconductor endures the magnetization process, enormous mechanical stresses are imposed on the bulk, which often leads to cracking. In the present work, we aim to resolve the viscous flux flow velocity v_0/w, i.e. v_0 (because w is a constant) and the stress distribution in a long rectangular slab superconductor for the decreasing external magnetic field (B_a) after zero-field cooling (ZFC) and field cooling (FC) using the Kim model and viscous flux flow equation simultaneously. The viscous flux flow velocity v_0/w and the magnetic field B^* at which the body forces point away in all of the slab volumes during B_a reduction, are determined by both B_a and the decreasing rate (db_a/dt) of the external magnetic field normalized by the full penetration field B_p. In previous studies, v_0/w obtained by the Bean model with viscous flux flow is only determined by db_a/dt, and the field B^* that is derived only from the Kim model is a positive constant when the maximum external magnetic field is chosen. This means that the findings in this paper have more physical contents than the previous results. The field $B^* < 0$ can be kept for any value of B_a when the rate db_a/dt is greater than a certain value. There is an extreme value for any curve of maximum stress changing with decreasing field B_a after ZFC if $B^* \leqslant 0$. The effect of db_a/dt on the stress is significant in the cases of both ZFC and FC.

Keywords: viscous flux flow velocity, external magnetic field, rate of external magnetic field, Kim model, stress, bulk superconductor

(Some figures may appear in colour only in the online journal)

1. Introduction

Superconducting bulks can be used as strong quasi-permanent magnets because of the capability of trapping a high magnetic field. The bulk magnets have potential for practical engineering application, such as superconducting motors [1], mixers [2], magnetic separation [3], drug delivery systems [4], magnetron sputtering devices [5], nuclear magnetic resonance [6], magnetic resonance imaging [7], and so on. The bulk superconductors are often magnetized in two ways: field cooled magnetization (FCM) using a superconducting coil magnet [6] and pulsed field magnetization (PFM) [8]. The FCM process is usually capable of trapping a higher magnetic field than PFM; for example, the world record trapped field of 17.6 T at 26 K in a disc-shaped GdBaCuO bulk pair has been achieved by using an 18 T superconducting magnet [9]. However, PFM is a promising technique for magnetizing the superconducting bulk because the compact and inexpensive experimental setup only uses a conventional solenoid magnet [10, 11]. During the FCM or PFM process, the Lorentz force due to the current-field interaction between

the induced persistent current and magnetic field results in the fracture behavior of the bulk, if the magnetic stress exceeds the fracture strength [12–14]. Bulk superconductors, such as (RE)BCO (where RE stands for a rare earth element, particularly, Y), have intrinsic brittleness due to the perovskite structure, and the strength and fracture toughness of the materials is low [15, 16]. The mechanical properties of bulk (RE)BCO are commonly evaluated by the tensile, compressive and bending tests at room and liquid nitrogen temperatures [17–22]. The tensile strength is about $30 \sim 70$ MPa [17, 18, 23–26] at the liquid nitrogen temperature. The flexural strength is slightly larger than the tensile strength [21, 22]. The average compressive strength has been reported by Murakami *et al* [20], and its value changes from 368 to 466 MPa at the liquid nitrogen temperature. This means that the compressive strength of superconducting bulk is over five times larger than the tensile strength at cryogenic temperature. The Lorentz force generated in the FCM or PFM process is applied to bulks as a tensile or compressive load. Because the compressive strength of superconducting bulks is much larger than the tensile strength, major cracking due to pinning-induced compressive stress has not been reported [27–30]. Before the large trapped magnetic fields are acquired, analysis of the tensile stress in bulks is very important in order to avoid serious damage to the samples when the bulks are excited by a magnetic field.

After a single crystal of $Bi_2Sr_2CaCu_2O_8$ was cooled under zero magnetic field, the magnetostriction of the bulk was measured along the *ab* plane by Ikuta *et al* [31] when the magnetic field was applied up to ± 6 T parallel to the *c* axis with a constant cyclic rate ($10\ \mathrm{mT\ S^{-1}}$). They found that the sample decreased in length during the magnetic field increasing process. Later, cracks under magnetic pressure at high trapped fields were studied by Ren *et al* [32], who found that the tensile stress appeared and a sample suffered damage when the applied magnetic field was ramped down. The present strain gauge method is useful for direct characterization of mechanical properties of large-grain bulk superconductors during the magnetization processes. After the samples had been cooled in the presence of 10 T at 50 K, Miyamoto *et al* [12] monitored the strains of large-grain Y-Ba-Cu-O and Sm-Ba-Cu-O bulks with several gauges mounted onto the sample surface when the external field was reduced from 10 to 0 T. Very recently, Takahashi *et al* [14] reported that the EuBaCuO ring bulk reinforced by a stainless steel ring was broken at the intermediate step of FCM from 8.3 T. They suggested that the actual fracture strength of the present ring bulk was between 50 and 59 MPa. In the theoretical aspect, the elastic responses of bulk superconductors shaped as a long rectangular slab or as circular or elliptic cylinders were respectively investigated for various stages of the magnetization process [33–35]. An exact solution of the full three-dimensional magnetoelastic problem was solved by Johansen, who presented the behavior of stress and strain in a long circular cylindrical superconductor [33] based on the Bean model and in a rectangular superconductor [34] based on the Bean and exponential models. Yong and Zhou [35] analyzed the stress and magnetostriction of an elliptic cylinder for a zero-field cooling (ZFC) process based on the Bean model. They found that the maximum stress of the semi-major axis was different from that of the semi-minor axis. The mechanical stresses and fracture behavior in a long circle cylinder or rectangular slab with a hole have also been investigated during the magnetization processes [36–40]. In addition, the stress distributions of bulk superconductors with constraining metal tubes were numerically evaluated [41, 42].

The above theoretical investigations solved the stress and magnetoelastic problems based on the critical state models. Those methods cannot contain the influence of the flux flow on the stress because the critical state models describe quasistatic flux distributions in bulk superconductors. The first investigation of time-dependent flux motion was undertaken by Anderson [43] who introduced the concept of flux creep. Later, Kim *et al* [44] pointed out that the motion of fluxoids was dominated by viscous effects at high flux velocities. The problem of incorporating viscous flux flow into the Bean model was first discussed by Melville [45], who argued that the motion of the magnetic fluxoids caused a small perturbation on the Bean flux profile. Two simple analytical solutions that satisfied both Bean and viscous flux flow equations simultaneously were presented and discussed by Liu and Bowden [46]. Employing viscous flux flow and critical state models, Inanir *et al* [47] calculated the magnetostriction for different frequencies of the applied magnetic field. They found that the presence of the viscous flux flow at high frequencies can considerably enhance the scale of the magnetostriction curves and also alter their shape. Considering the flux creep, Xue *et al* [48] analyzed the effect of both the viscous flux flow and thermally activated flux creep on the magnetostriction and the internal tensile stress for a long rectangular superconducting slab. Feng and Gao [49] studied the magnetoelastic problem of an isotropic hollow superconducting cylinder subjected to the applied descending magnetic field, where the flux creep and viscosity flow existed simultaneously. In our previous works, the viscous flux flow velocity υ_0/w or υ_0/R, i.e. υ_0 (because w and R are two constants) and the stress distributions in bulk superconductors shaped as a long rectangular slab and a circular cylinder had been respectively investigated using the Bean model with viscous flux flow after ZFC and field cooling (FC) [29, 50–52]. The calculations in our previous studies revealed that the viscous flux flow velocity and the stress distributions were remarkably impacted by db_a/dt. However, the method that combines the Kim model and viscous flux flow to study the flux motion and the distributions of stress has not been reported so far. The critical current density (J_c) in the Bean model is a constant and independent from the magnetic field. The effect of the external magnetic field on viscous flux flow velocity has not been revealed using the Bean model and viscous flux flow equation simultaneously. Compared with the Bean model, the Kim model would be more physical since

the critical current density varies with the magnetic flux density. Some interesting results can be obtained by using the Kim model and viscous flux flow to solve the magnetoelastic problem of bulk superconductors.

The compressive stress is produced during the magnetic field increasing process [31, 50, 52], however, the tensile stress appears as the applied magnetic field is ramped down [32–34]. The study of tensile stress in superconducting bulks is key to avoid cracking during the magnetization process. In this paper, we employed the Kim model and viscous flux flow simultaneously and the influences of the external magnetic field and its rate on both the viscous flux flow velocity and the tensile stress in a long rectangular slab superconductor have been investigated during the external magnetic field decreasing process after ZFC and FC.

2. General equations

A bulk superconductor shaped as a rectangular slab with a thickness of $2w$ ($-w < x < w$) and infinity along the y- and z-directions is placed in an external magnetic field (B_a) pointing in the z direction. The slab is assumed to be isotropic and demagnetization effects are neglected. Similar to the method of Inanir *et al* [47], the distribution of magnetic flux density in an infinite superconducting slab for the Kim model with a mean flux velocity $\upsilon(t)$ obeys the following equation,

$$\frac{\partial B(x,\ t)}{\partial x} = \mp\mu_0\left(J_C(x,\ t) + \frac{\eta}{\phi_0}\upsilon(t)\right), \tag{1}$$

where μ_0 is magnetic permeability in the vacuum, $B(x,\ t)$ is the total magnetic field in the slab, η is the viscosity associated with flux motion, $\upsilon(t)$ is the local flux velocity, and ϕ_0 is the flux quantum. The $\mp$ signs are used for flux motion into (out of) the superconductor with increasing (decreasing) external magnetic fields, respectively, $J_C(x,\ t)$ is the critical current density in the Kim model and $a_c/J_c(x,\ t)$ can be written as a power series expansion about the total magnetic field $B(x,\ t)$ in general [53, 54]. During the magnetization at critical states, a linear distribution is adopted in [28, 55]. So $J_C(x,\ t)$ in the paper is expressed as follows,

$$J_C(x,\ t) = \mp\frac{a_c}{|B(x,\ t)| + B_0}. \tag{2}$$

The sign is determined by the slope of flux density in the slab and a_c and B_0 are two positive parameters.

The equation of flux continuity is given by [46]

$$B\upsilon = \frac{\partial}{\partial t}\int_x^{+\infty} B(x',\ t)dx'. \tag{3}$$

Following Liu and Bowden [46], we assume that $B(x,\ t) = B(x - \upsilon_0 t)$, where υ_0 is a constant flux velocity. Putting the solution and equation (2) into equation (1), we obtain

$$\frac{B(x,\ t)}{\upsilon_0\eta\mu_0}\phi_0 - \frac{a_c\phi_0^2}{\upsilon_0^2\eta^2\mu_0}\ln\left(B(x,\ t) + B_0 + \frac{a_c\phi_0}{\upsilon_0\eta}\right) = \mp(x - \upsilon_0 t). \tag{4}$$

Equation (4) is an implicit function about the total magnetic field $B(x,\ t)$ in the superconducting bulk. If $x = w$ in equation (4), $B(w,\ t)$ equals the external magnetic field $B_a(t)$. When $B_a(t)$ decreases from its maximum value B_M, the implicit expression of $B_a(t)$ is given by,

$$\frac{B_a(t) - B_M}{\upsilon_0\eta\mu_0}\phi_0 - \frac{a_c\phi_0^2}{\upsilon_0^2\eta^2\mu_0}\ln\left(\frac{B_a(t) + B_0 + \frac{a_c\phi_0}{\upsilon_0\eta}}{B_M + B_0 + \frac{a_c\phi_0}{\upsilon_0\eta}}\right) = -\upsilon_0 t, \tag{5}$$

where the negative sign on the right-hand side denotes the external magnetic field decreasing process.

A solution for the stress in a long rectangular slab placed in the parallel applied magnetic field has been presented by Johansen [34] using the plane strain approach [56]. The evaluation of the stress in the thickness direction is given by [28, 29, 34]

$$\sigma_x(x,\ t) = -\frac{1}{2\mu_0}[B_a^2(t) - B^2(x,\ t)]. \tag{6}$$

The Kim model full penetration field can be expressed as [28]

$$B_p = \sqrt{B_0^2 + 2\mu_0 a_c w} - B_0. \tag{7}$$

For simplifying the discussion, the parameter p is introduced to reduce the number of variables [28],

$$p = \frac{\sqrt{2\mu_0 a_c w}}{B_0}. \tag{8}$$

All the stresses in the study are normalized by $\sigma_0 = B_p^2/(2\mu_0)$.

3. Decreasing field after ZFC

After the bulk superconductor has cooled in the absence of the magnetic field, the applied magnetic field increases from $B_a = 0$ to $B_M = 4B_p$. It is assumed that the critical current fills the entire slab as $B_a = B_M$. When the applied field is swept down from B_M, the flux profiles are divided into active and non-active parts at the point x_0. The direction of the critical currents remains the same in the non-active part ($0 < x < x_0$) and is reversed in the active part ($x_0 < x < w$). The implicit expression of x_0 can be obtained,

$$\frac{B_a(t) - \sqrt{(B_M + B_0)^2 - 2\mu_0 a_c(w - x_0)} + B_0}{\upsilon_0\eta\mu_0}\phi_0 + \frac{a_c\phi_0^2}{\upsilon_0^2\eta^2\mu_0}\ln\frac{\sqrt{(B_M + B_0)^2 - 2\mu_0 a_c(w - x_0)} + \frac{a_c\phi_0}{\upsilon_0\eta}}{B_a(t) + B_0 + \frac{a_c\phi_0}{\upsilon_0\eta}} = x_0 - w. \tag{9}$$

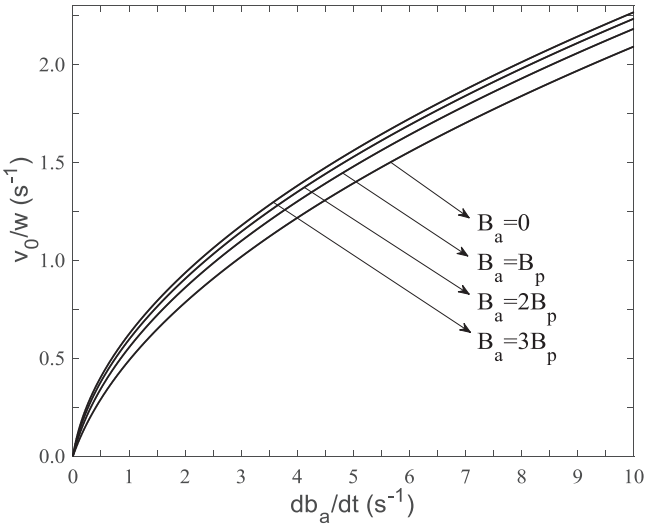

Figure 1. The viscous flux flow velocity υ_0/w changes with the rate db_a/dt under the different values of external magnetic field B_a.

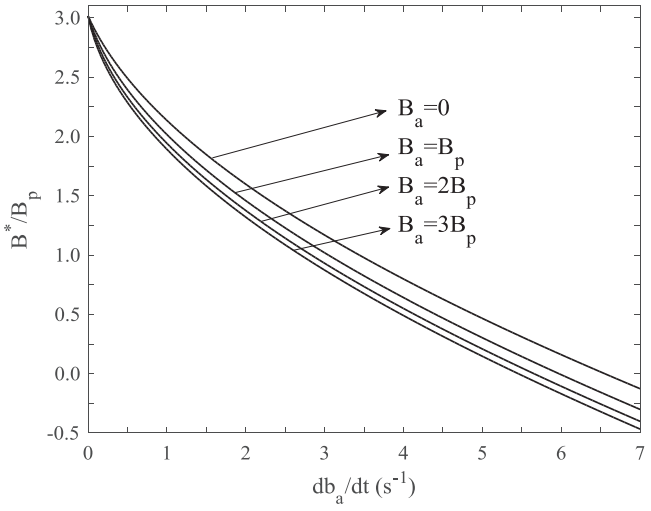

Figure 2. The db_a/dt dependence of the magnetic field B^* under the different values of the external magnetic field B_a.

Based on equation (5), the decreasing rate db_a/dt of the external magnetic field normalized by B_p can be given by

$$\left|\frac{db_a(t)}{dt}\right| = \left|\frac{dB_a(t)/B_p}{dt}\right| = \left(\frac{p^2}{2(\sqrt{1+p^2}-1)^2\left(\frac{B_a(t)}{B_p}+\frac{1}{\sqrt{1+p^2}-1}\right)} + \frac{p}{\sqrt{2}(\sqrt{1+p^2}-1)}\frac{\eta}{\phi_0}\sqrt{\frac{\mu_0 w}{a_c}}\upsilon_0\right)\frac{\upsilon_0}{w}. \quad (10)$$

In order to simplify the discussion and reduce the number of parameters, $\sqrt{\mu_0 w/a_c}\eta\upsilon_0/\phi_0 = \upsilon_0/w$ is assumed. As known from equation (10), the viscous flux flow velocity υ_0/w, i.e. υ_0 (because w is a constant), is determined by db_a/dt, B_a and the parameter p. However, υ_0/w obtained by the Bean model with the viscous flux flow is only determined by db_a/dt [29].

Figure 1 shows the relationship between the viscous flux flow velocity υ_0/w and the rate db_a/dt of the applied field normalized by B_p under the different values of the external magnetic field B_a. It can be seen from figure 1 that υ_0/w increases with increasing db_a/dt. When the external magnetic field B_a decreases, υ_0/w decreases for the same $db_a/$dt. Furthermore, υ_0/w for the identical db_a/dt decreases more remarkably as B_a changes from B_p to 0 than that when B_a changes from $3B_p$ to $2B_p$ (or from $2B_p$ to B_p). This means that the external magnetic field significantly influences the viscous flux flow velocity as B_a is less than or equal to B_p. The effect of the parameter p on υ_0/w cannot be discussed by equation (10). The following explanations can understand the viewpoint; $B_p = (\sqrt{p^2+1}-1)B_0$ can be obtained by equations (7) and (8) while db_a/dt is a function of dB_a/dt normalized by B_p. This means that db_a/dt changes with the parameter p. As known from equation (10), υ_0/w is related to db_a/dt, B_a and the parameter p. So the relationship between υ_0/w and parameter p is not evident. In the calculations, $p = 1$ is adopted. Additionally, the parameter p dependence of the stress cannot be studied in this paper because the different values of parameter p give the different values of σ_0.

The field B^* is the magnetic field at which the body forces point away in all the slab volumes during the external magnetic field reduction. Considering the Kim model with the viscous flux flow, the field B^* can be obtained by the following implicit expression,

$$\frac{B^* - \sqrt{(B_M+B_0)^2 - 2\mu_0 a_c w} + B_0}{\upsilon_0\eta\mu_0}\phi_0 + \frac{a_c\phi_0^2}{\upsilon_0^2\eta^2\mu_0}\ln\frac{\sqrt{(B_M+B_0)^2-2\mu_0 a_c w} + \frac{a_c\phi_0}{\upsilon_0\eta}}{B^*+B_0+\frac{a_c\phi_0}{\upsilon_0\eta}} = -w. \quad (11)$$

As known from expression (8) of B^* derived from the Kim model in [28], the field B^* is only determined by the maximum external magnetic field B_M. It can be seen from equation (11) that B^* is related to B_M and flux flow velocity υ_0. As shown in figure 1, the rate db_a/dt and external magnetic field B_a influences the viscous flux flow velocity υ_0/w, and, therefore, affects the field B^*. In order to clarify the effects of db_a/dt and B_a on the field B^*, the relationship between B^* and $db_a/$dt with the different values of B_a is shown in figure 2. At one external magnetic field B_a, the field B^* rapidly decreases with increasing db_a/dt. If the rate db_a/dt stays constant, the field B^* increases with decreasing B_a. As

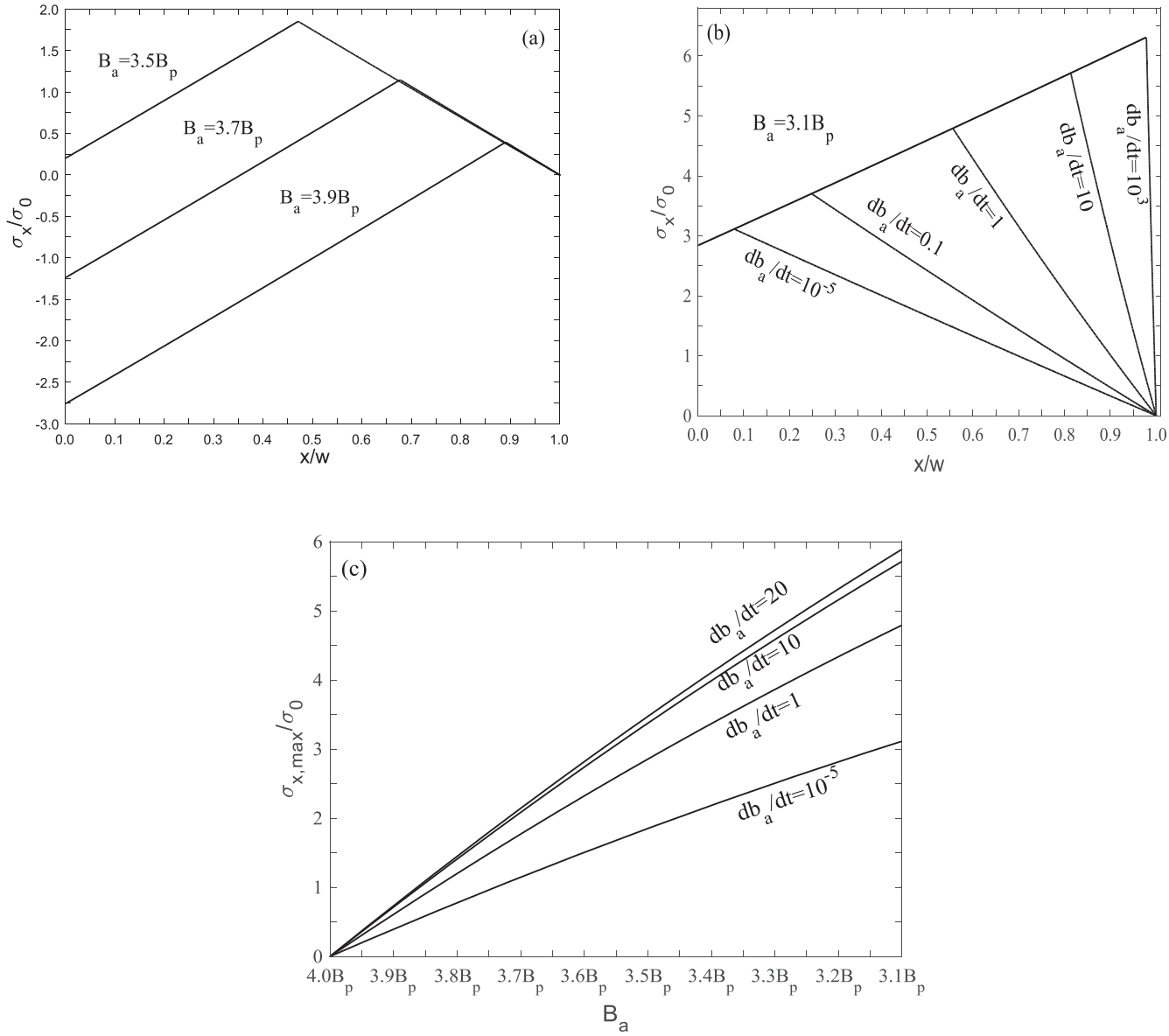

Figure 3. (a) Stress profiles as the applied field is decreased from $4B_p$ to $3.9B_p$, $3.7B_p$, and $3.5B_p$ for $db_a/dt = 10^{-5}$ s^{-1}. (b) Stress profiles as the applied field is decreased from $4B_p$ to $3.1B_p$ for different values of db_a/dt (s^{-1}). (c) The maximum stress versus the applied field with the different values of db_a/dt (s^{-1}).

shown in figure 2, the field $B^* \leqslant 0$ for $B_a = 0$ if $db_a/dt \geqslant 6.55$ s^{-1}, for $B_a = B_p$ if $db_a/dt \geqslant 5.97$ s^{-1}, for $B_a = 2B_p$ if $db_a/\mathrm{dt} \geqslant 5.66$ s^{-1}, and for $B_a = 3B_p$ if $db_a/dt \geqslant 5.46$ s^{-1}. This means that the field B^* for a constant value of B_a has an opposite direction when the rate db_a/dt is greater than a certain value. So the discussions of stress distributions should be divided into two cases that are $B^* > 0$ and $B^* \leqslant 0$.

3.1. The case of $B^* > 0$

In this case, there are two stages that are $B_M > B_a > B^* > 0$ ($x_0 > 0$) and $B^* > B_a \geqslant 0$ ($x_0 = 0$) as the external magnetic field decreases from B_M to B_a.

3.1.1. Stage 1: $B_M > B_a > B^* > 0$. In this stage, the values of x_0 are always greater than 0. From equation (1), the magnetic field in the superconducting slab can be obtained,

$$\begin{cases} B(x,t) = \sqrt{(B_M + B_0)^2 - 2\mu_0 a_c (w - x)} - B_0 & 0 \leqslant x \leqslant x_0 \\ \dfrac{B_a(t) - B(x,t)}{\upsilon_0 \eta \mu_0 w}\phi_0 + \dfrac{a_c \phi_0^2}{\upsilon_0^2 \eta^2 \mu_0 w} \ln \dfrac{B(x,t) + B_0 + \frac{a_c \phi_0}{\upsilon_0 \eta}}{B_a(t) + B_0 + \frac{a_c \phi_0}{\upsilon_0 \eta}} = -\left(1 - \dfrac{x}{w}\right) & x_0 \leqslant x \leqslant w \end{cases}. \tag{12}$$

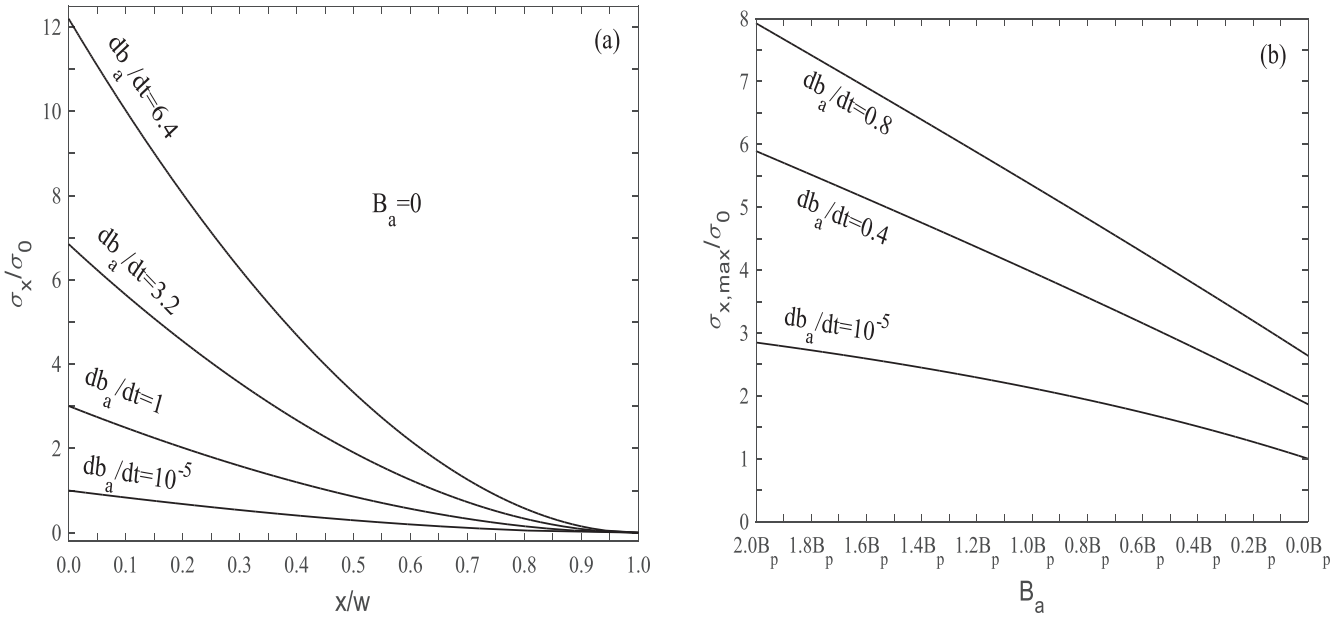

Figure 4. (a) Stress profiles with the different values of db_a/dt (s^{-1}) as the applied field deceases from $4B_p$ to 0. (b) The maximum stress versus the applied field with the different values of db_a/dt (s^{-1}).

As known from equation (12), the magnetic field $B(x,\ t)$ in the active part cannot be written in the form of explicit expression and contains the viscous flux flow terms. It is distinguished from the results obtained using only the Kim model [28].

When the rate of the applied field is very small ($db_a/dt = 10^{-5}\ s^{-1}$), the stress distribution is shown in figure 3(a). Compared with the results obtained using only the Kim model [28], we find that the curves of the stress with respect to x/w are almost the same because the flux motion is quasistatic as $db_a/dt = 10^{-5}\ s^{-1}$. Figure 3(b) shows the distribution of stress with the different db_a/dt as the applied field is decreased from $4B_p$ to $3.1B_p$. As shown in figure 3(b), the stress increases with increasing x/w first, up to the maximum, and then decreases. The point x_0 where the field gradient changes sign and the maximum tensile stress appears increases with increasing db_a/dt. The effect of db_a/dt on the stress is appreciable. With increasing db_a/dt, the stress in the remagnetization region ($x_0 \leqslant x < w$) increases and stays the same in the non-active region ($0 \leqslant x < x_0$). The relationship between maximum tensile stress and applied field reducing from $4B_p$ to $3.1B_p$ is illustrated in figure 3(c). As can be seen from figure 3(c), the maximum tensile stress increases with decreasing external magnetic field B_a. Furthermore, the maximum stress at the same external magnetic field rapidly increases as db_a/dt increases from $10^{-5}\ s^{-1}$ to $10\ s^{-1}$ and slightly increases as db_a/dt increases from $10\ s^{-1}$ to $20\ s^{-1}$.

3.1.2. Stage 2: $\boldsymbol{B^* > B_a \geqslant 0}$. As the applied field is decreased from B_M to $B^* > B_a \geqslant 0$, x_0 is equal to zero and the entire superconducting slab is activated by the applied magnetic field. The flux density distribution in the superconducting slab in the x direction can be expressed as follows,

$$\frac{B_a(t) - B(x,\ t)}{\upsilon_0 \eta \mu_0 w}\phi_0 + \frac{a_c \phi_0^2}{\upsilon_0^2 \eta^2 \mu_0 w} \ln \frac{B(x,\ t) + B_0 + \dfrac{a_c \phi_0}{\upsilon_0 \eta}}{B_a(t) + B_0 + \dfrac{a_c \phi_0}{\upsilon_0 \eta}} = -\left(1 - \frac{x}{w}\right) \quad 0 < x < w. \tag{13}$$

Figure 4(a) plots the stress distribution with the different values of db_a/dt as the applied field deceases from $4B_p$ to 0. As known from the discussions regarding figure 2, $db_a/dt < 6.55\ s^{-1}$ must be ensured in order to keep $B^* > 0$ as $B_a = 0$. It is observed that the stress is tensile and all maximum stresses for different db_a/dt appear at the center of the superconductor bulk. With increasing db_a/dt, the tensile stress increases at any position and the stress curve gets steeper and steeper. As shown in figure 4(a), $\sigma_{T,x=0} \approx \sigma_0$ as $db_a/dt = 10^{-5}\ s^{-1}$, $\sigma_{T,x=0} \approx 3.01\sigma_0$ as $db_a/dt = 1\ s^{-1}$, $\sigma_{T,x=0} \approx 6.85\sigma_0$ as $db_a/dt = 3.2\ s^{-1}$, and $\sigma_{T,x=0} \approx 12.20\sigma_0$ as $db_a/dt = 6.4\ s^{-1}$. This means that the effect of db_a/dt on the maximum stress is significant during this stage because the body force is only tensile in the entire slab. The superconductor bulk suffers the risk of damage when the applied field drops to small values with a large db_a/dt after ZFC. To further comprehend the phenomenon, figure 4(b) shows that the maximum tensile stress varies with the applied magnetic field under the different values of db_a/dt. It can be seen from figure 4(b), that the tensile maximum stress decreases with decreasing applied field B_a. So the tendencies of the curves in figure 4(b) are contrary to those in figure 3(c). Moreover, the maximum tensile stress increases at any external magnetic field with increasing db_a/dt.

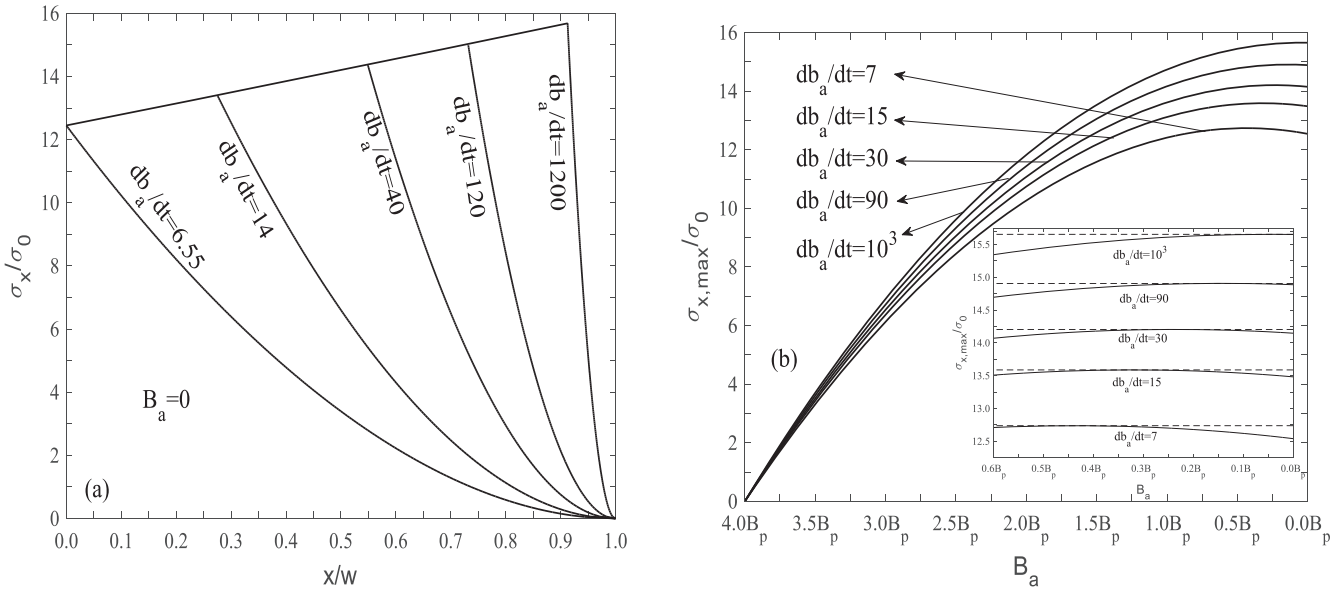

Figure 5. (a) Stress profiles with the different values of db_a/dt (s^{-1}) as the applied field deceases from $4B_p$ to 0. (b) The relationship between maximum stress and the applied field B_a changing from $4B_p$ to 0 with the different values of db_a/dt (s^{-1}). The inset is the relationship between maximum stress and B_a varying from $0.6B_p$ to 0 with the different values of db_a/dt (s^{-1}).

3.2. The case of $B^* \leqslant 0$

In this case, the magnetic flux density distribution in the superconducting slab along the x direction can be expressed by equation (12). Figure 5(a) plots the stress distributions with the different values of db_a/dt as the applied field deceases from $4B_p$ to 0. As shown in figure 5(a), x_0 appears when $db_a/dt > 6.55\ s^{-1}$, and the stress in the remagnetization region ($x_0 \leqslant x < w$) increases with increasing db_a/dt. Figure 5(b) illustrates the relationship between maximum tensile stress and applied magnetic field B_a under the different values of db_a/dt. It can be seen from figure 2 that $B^* < 0$ can be retained for any B_a varying from $4B_p$ to 0 when $db_a/dt > 6.55\ s^{-1}$. As shown in figure 5(b), there is an extreme value for any curve of maximum stress changing with B_a. In order to show this phenomenon clearly, the inset of figure 5(b) shows an enlarged drawing where the extreme values emerge. When B_a decreases from $4B_p$ to 0, the maximum stress increases first, up to the extreme value, and then decreases. The extreme values of $\sigma_{x,\,max}/\sigma_0$ are 12.74 for $db_a/dt = 7\ s^{-1}$ at $B_a = 0.44B_p$, 13.59 for $db_a/dt = 15\ s^{-1}$ at $B_a = 0.33B_p$, 14.21 for $db_a/dt = 30\ s^{-1}$ at $B_a = 0.23B_p$, 14.91 for $db_a/dt = 90\ s^{-1}$ at $B_a = 0.19B_p$, and 15.66 for $db_a/dt = 10^3\ s^{-1}$ at $B_a = 0.05B_p$. This means that the dependences of the maximum stress on B_a are not monotonic if $B^* \leqslant 0$. In addition, the maximum stress increases with increasing db_a/dt at any external magnetic field.

4. Decreasing field after FC

Field cooling is a useful method to accomplish the magnetization of bulk superconductors. The cooling field B_{fc} is also equal to the flux density frozen in the superconductor when the field is swept down. The flux density distribution is given by

$$\begin{cases} B(x,\,t) = B_{fc} & 0 < x < x_0 \\ \dfrac{B_{\rm a}(t) - B(x,\,t)}{\upsilon_0\eta\mu_0 {\rm w}}\phi_0 + \dfrac{a_c\phi_0^2}{\upsilon_0^2\eta^2\mu_0 w}\ln\dfrac{B(x,\,t) + B_0 + \frac{a_c\phi_0}{\upsilon_0\eta}}{B_{\rm a}(t) + B_0 + \frac{a_c\phi_0}{\upsilon_0\eta}} = -\left(1 - \dfrac{x}{w}\right) & x_0 < x < w \end{cases}. \tag{14}$$

x_0 can be obtained

$$x_0 = \frac{B_{\rm a}(t) - B_{fc}}{\upsilon_0\eta\mu_0}\phi_0 + \frac{a_c\phi_0^2}{\upsilon_0^2\eta^2\mu_0}\ln\frac{B_{fc} + B_0 + \frac{a_c\phi_0}{\upsilon_0\eta}}{B_{\rm a}(t) + B_0 + \frac{a_c\phi_0}{\upsilon_0\eta}} + w. \tag{15}$$

$B_a\,(t)$ is given by

$$\frac{B_a(t) - B_{fc}}{\upsilon_0\eta\mu_0}\phi_0 - \frac{a_c\phi_0^2}{\upsilon_0^2\eta^2\mu_0}\ln\left(\frac{B_a(t) + B_0 + \frac{a_c\phi_0}{\upsilon_0\eta}}{B_{fc} + B_0 + \frac{a_c\phi_0}{\upsilon_0\eta}}\right) = -\upsilon_0 t. \tag{16}$$

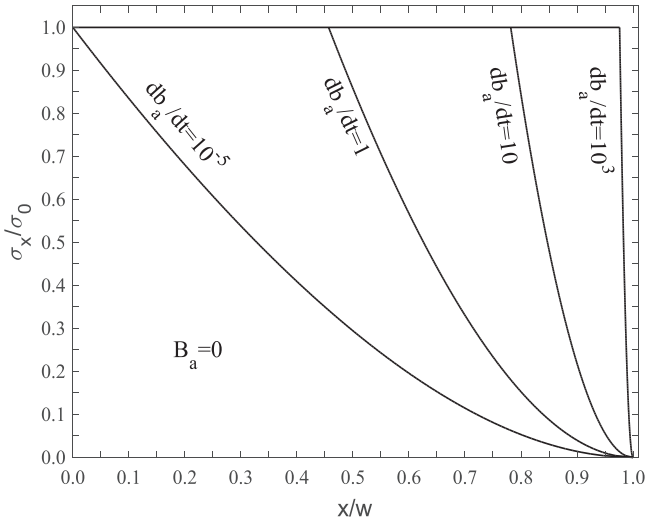

Figure 6. Stress distributions with the different values of db_a/dt (s^{-1}) as the external magnetic field decreases from $B_{fc} = B_P$ to the remanent state ($B_a = 0$) after FC.

When the applied field B_a decreases from $B_{fc} = B_p$ to the remanent state ($B_a = 0$), the stress distributions along the x direction with the different values of db_a/dt are plotted in figure 6. With increasing db_a/dt, x_0 moves away from the center of the superconductor and stress in the remagnetization region increases. The maximum tensile stress stays constant as $db_a/dt > 10^{-5}\,s^{-1}$. These results are similar to those obtained by the Bean model with viscous flux flow [29].

5. Conclusions

In this paper, the viscous flux flow velocity v_0/w and the stress distributions in a long rectangular slab superconductor have been resolved by the Kim model with viscous flux flow for the decreasing applied field after ZFC and FC. The results show that the effect of db_a/dt on the stress is significant in the case of both ZFC and FC. Compared with our previous studies [29, 50–52] and the results derived only from the Kim model [28], some new results and conclusions are summarized as follows.

(1) The viscous flux flow velocity v_0/w and the field B^* at which the body forces point away in all the slab volumes during the external magnetic field reduction are determined by both B_a and db_a/dt.
(2) The field $B^* < 0$ can be retained for any B_a varying from $4B_p$ to 0 when $db_a/dt > 6.55\,s^{-1}$.
(3) There is an extreme value for any curve of maximum stress changing with the decreasing field B_a after ZFC if $B^* \leqslant 0$.

Although some investigators consider the validity of the Bean model is questionable for an extensive analysis of the elastic behavior [28, 30], to our knowledge, no research has been carried out to confirm that the mechanical properties calculated by the Kim model are more accurate than those using the Bean model. As found from our calculations, the more physical contents are revealed by the Kim model combining with the viscous flux flow, such as the effect of B_a on v_0/w and new features of the field B^*.

Acknowledgment

This work was supported by the National Natural Science Foundation of China (Grant No. 11572232).

ORCID iDs

Yong Yang https://orcid.org/0000-0002-5064-0722

References

[1] Huang Z, Zhang M, Wang W and Coombs T A 2014 *IEEE Trans. Appl. Supercond.* **24** 4602605
[2] Koyama F, Akiyama S and Murakami M 2006 *Supercond. Sci. Technol.* **19** S572
[3] Yokoyama K, Oka T, Okada H and Noto K 2003 *Physica* C **392–396** 739
[4] Sahoa N, Nishijima N, Tanaka H and Sasaki A 2009 *Physica* C **469** 1286
[5] Yanagi Y, Matsuda T, Hazama H, Yokouchi K, Yoshikawa M, Itoh Y, Oka T, Ikuta H and Mizutani U 2005 *Physica* C **426–431** 764
[6] Nakamura T, Itoh Y, Yoshikawa M, Oka T and Uzawa J 2007 *Concept Magn. Reson. (Magn. Reson. Eng.)* **31B** 65
[7] Ogawa K, Nakamura T, Terada Y, Kose K and Haishi T 2011 *Appl. Phys. Lett.* **98** 234101
[8] Fujishiro H and Naito T 2010 *Supercond. Sci. Technol.* **23** 105021
[9] Durrell J H *et al* 2014 *Supercond. Sci. Technol.* **27** 082001
[10] Mochizuki H, Fujishiro H, Naito T, Itoh Y, Yanagi Y and Nakamura T 2016 *IEEE Trans. Appl. Supercond.* **26** 6800205
[11] Yang X B, Li X H, He Y F, Wang X J and Xu B 2017 *Physica* C **535** 1
[12] Miyamoto T, Nagashima K, Sakai N and Murakami M 2000 *Physica* C **340** 41
[13] Fujishiro H, Ainslie M D, Takahashi K, Naito T, Yanagi Y, Itoh Y and Nakamura T 2017 *Supercond. Sci. Technol.* **30** 085008
[14] Takahashi K, Fujishiro H, Naito T, Yanagi Y, Itoh Y and Nakamura T 2017 *Supercond. Sci. Technol.* **30** 115006
[15] Cook R F, Dinger T R and Clarke D R 1987 *Appl. Phys. Lett.* **51** 454
[16] Fujimoto H 2009 *IEEE Trans. Appl. Supercond.* **19** 2933
[17] Katagiria K, Murakami A, Shoji Y, Teshima H, Sawamura M, Iwamoto A, Mito T and Murakami M 2004 *Physica* C **412–414** 633
[18] Kasaba K, Katagiri K, Murakami A, Sato G, Sato T, Murakami M, Sakai N, Teshima H and Sawamura M 2005 *Physica* C **426–431** 639
[19] Kan R, Katagiri K, Murakami A, Kasaba K, Shoji Y, Noto K, Sakai N and Murakami M 2004 *IEEE Trans. Appl. Supercond.* **14** 1114
[20] Murakami A, Katagiri K, Kan R, Miyata H, Shoji Y, Noto K, Iwamoto A and Mito T 2005 *Physica* C **426–431** 644

[21] Katagiri K, Hatakeyama Y, Sato T, Kasaba K, Shoji Y, Murakami A, Teshima H and Hirano H 2006 *Physica* C **445–448** 631
[22] Fujimoto H, Murakami A, Teshima H and Morita M 2013 *Cryogenics* **57** 6
[23] Schatzle P, Krabbes G, Gruss S and Fuchs G 1999 *IEEE Trans. Appl. Supercond.* **9** 2022
[24] Lee D and Salama K 1990 *Japan. J. Appl. Phys.* **29** L2017
[25] Miyamoto T, Katagiri J, Nagashima K and Murakami M 1999 *IEEE Trans. Appl. Supercond.* **9** 2066
[26] Matsui M, Sakai N and Murakami M 2002 *Supercond. Sci. Technol.* **15** 1092
[27] Johansen T H 2000 *Supercond. Sci. Technol.* **13** R121
[28] Yong H D and Zhou Y H 2008 *J. Appl. Phys.* **103** 113903
[29] Yang Y, Xiao L Y and Li X H 2010 *J. Appl. Phys.* **107** 023910
[30] Zeng J, Wang X G, Wu H P, Xue F and Zhu J 2016 *AIP Adv.* **6** 075305
[31] Ikuta H, Hirota N, Nakayama Y, Kishio K and Kitazawa K 1993 *Phys. Rev. Lett.* **70** 2166
[32] Ren Y, Weinstein R, Liu J, Sawh R P and Foster C 1995 *Physica* C **251** 15
[33] Johansen T H 1999 *Phys. Rev.* B **60** 9690
[34] Johansen T H 1999 *Phys. Rev.* B **59** 11187
[35] Yong H D and Zhou Y H 2013 *J. Appl. Phys.* **114** 023902
[36] Johansen T H, Wang C, Chen Q Y and Chu W-K 2000 *J. Appl. Phys.* **88** 2730
[37] Zeng J, Zhou Y H and Yong H D 2009 *Physica* C **469** 822
[38] Zhou Y H and Yong H D 2007 *Phys. Rev.* B **76** 094523
[39] Gao Z W and Zhou Y H 2008 *Supercond. Sci. Technol.* **21** 095010
[40] Feng W J, Gao S W and Li Y S 2016 *Appl. Math. Modelling* **40** 2529
[41] Yang X B and Tu S T 2012 *J. Appl. Phys.* **112** 023909
[42] Tsuchimoto M and Morita M 2016 *Phys. Procedia* **81** 170
[43] Anderson P W 1962 *Phys. Rev. Lett.* **9** 309
[44] Kim Y B, Hempstead C F and Strnad A R 1964 *Rev. Mod. Phys.* **36** 43
Kim Y B, Hempstead C F and Strnad A R 1965 *Phys. Rev.* **139A** 1163
[45] Melville P H 1972 *Phys. Lett.* **39A** 373
[46] Liu Z and Bowden G J 1991 *Supercond. Sci. Technol.* **4** 122
[47] Inanir F, Celebi S, Altunbas M, Okutan M and Erdogan M 2007 *Physica* C **459** 11
[48] Xue F, Yong H-D and Zhou Y-H 2010 *J. Appl. Phys.* **108** 103910
[49] Feng W J and Gao S W 2014 *Physica* C **500** 14
[50] Yang Y, Xiao L Y, Li X H and Zhang G-M 2010 *IEEE Trans. Appl. Supercond.* **20** 1507
[51] Yang Y, Zhang G M, Wang L, Hua Z Q and Li T 2011 *Supercond. Sci. Technol.* **24** 095003
[52] Yang Y and Zheng X J 2015 *J. Supercond. Nov. Magn.* **28** 2255
[53] Kim Y B, Hempstead C F and Strnad A R 1962 *Phys. Rev. Lett.* **9** 306
[54] Hilton D K, Gavrilin A V and Trociewitz U P 2015 *Supercond. Sci. Technol.* **28** 074002
[55] Kim Y B, Hempstead C F and Strnad A R 1963 *Phys. Rev.* **129** 528
[56] Timoshenko S and Goodier J N 1951 *Theory of Elasticity* (New York: McGraw-Hill)